The influence of early-life adversity on the coupling of structural and functional brain connectivity across childhood

Shi Yu Chan [1]✉, Zhen Ming Ngoh [1], Zi Yan Ong [1], Ai Ling Teh[1,2], Michelle Z. L. Kee [1], Juan H. Zhou [3,4], Marielle V. Fortier[1,5,6], Fabian Yap[6,7,8], Julia L. MacIsaac[9], Michael S. Kobor[9,10], Patricia P. Silveira [3,11], Michael J. Meaney[1,3,11,12] & Ai Peng Tan [1,3,12,13]✉

Early-life adversity (ELA) exposure is suggested to accelerate development. However, the influence of ELA on neurodevelopmental trajectories has not been assessed directly but largely inferred from retrospective reporting in adult cohorts. Using multimodal neuroimaging data from a pediatric cohort study ($N = 549$), we modeled neurodevelopmental trajectories over childhood with structure–function coupling (SC–FC), the correlation between structural and functional connectivity. A linear decrease in SC–FC was observed from age 4.5 to 7.5 years. When stratified by ELA, only the high-adversity group showed a curvilinear trajectory, with a steep decrease between age 4.5 and 6 years, suggestive of accelerated neurodevelopment. This finding was confirmed by increased DNA-derived epigenetic age acceleration at age 6 years in the high- relative to low-adversity groups. SC–FC at age 4.5 years also positively moderated the associations between ELA and behavioral outcomes assessed in mid-childhood. These results demonstrate the association between ELA and neurodevelopment, and how they interact to influence behavior.

Exposure to early-life adversity (ELA) is a risk factor for behavioral and emotional problems in childhood as well as long-term health consequences[1]. Neuroimaging studies provide a wealth of evidence for the association of perinatal adversity with neurodevelopmental outcomes[2,3]. These findings include alterations in structure and connectivity in brain regions that are implicated in common mental disorders. The association of ELA with structural and functional development of the brain[4] is now thought to represent adversity-related adaptations rather than stress-induced damage. ELA serves as a signal of the prevailing environmental conditions that influence the pace of brain development as an

[1]Singapore Institute for Clinical Sciences (SICS), Agency for Science, Technology and Research (A*STAR), Singapore, Singapore. [2]Bioinformatics Institute, Agency for Science, Technology and Research (A*STAR), Singapore, Singapore. [3]Yong Loo Lin School of Medicine, National University of Singapore (NUS), Singapore, Singapore. [4]Department of Electrical and Computer Engineering, National University of Singapore, Singapore, Singapore. [5]Department of Diagnostic and Interventional Imaging, KK Women's and Children's Hospital, Singapore, Singapore. [6]Duke–NUS Medical School, Singapore, Singapore. [7]Department of Paediatrics, KK Women's and Children's Hospital, Singapore, Singapore. [8]Lee Kong Chian School of Medicine, Nanyang Technological University, Singapore, Singapore. [9]Centre for Molecular Medicine and Therapeutics, University of British Columbia, Vancouver, British Columbia, Canada. [10]Child and Brain Development Program, Canadian Institute for Advanced Research (CIFAR), Toronto, Ontario, Canada. [11]Department of Psychiatry and Douglas Mental Health University Institute, McGill University, Montreal, Québec, Canada. [12]Brain–Body Initiative Program, Agency for Science, Technology and Research (A*STAR), Singapore, Singapore. [13]Department of Diagnostic Imaging, National University Health System, Singapore, Singapore. ✉e-mail: chan_shi_yu@sics.a-star.edu.sg; dnrtanap@nus.edu.sg

adaptive response to match the demands of unfavorable developmental conditions, at the potential cost to adult well-being[5]. In a compromised environment, accelerating development to achieve independence may be prioritized over extended neuroplasticity that benefits the development of higher brain function[6]. The 'stress acceleration' hypothesis proposes that exposure to ELA accelerates development, especially in fear/stress-related domains and emotion circuits[7]. Rodents raised in stressful environments show accelerated development of fear learning and memory retention[8,9]. In humans, children exposed to maternal distress and deprivation show adult-like limbic brain features (for example, larger amygdala volumes, functional connectivity patterns typically observed in adults)[10–12]. Moreover, children exposed to early-life stress show accelerated biological age measured via either telomere length or DNA methylation-derived epigenetic age[13,14].

The current literature on ELA and neurodevelopmental trajectories is limited by a lack of longitudinal neuroimaging data during childhood that are required for a within-subject assessment of the developmental acceleration hypothesis. Most adversity-related studies with large neuroimaging datasets are retrospective cross-sectional studies where the neuroimaging data are collected in adults reporting on adverse childhood experiences (ACE). Therefore, developmental trajectories are not assessed directly but are inferred based on adult data. In addition, existing neurodevelopmental cohorts (for example, the Adolescent Brain Cognitive Development (ABCD), Human Connectome Project Development (HCP-D) and Pediatric Imaging, Neurocognition, and Genetics (PING) studies) cover large age ranges with few subjects below age 7 years, possibly due to the challenges of collecting high-quality neuroimaging data in preschool children. Thus, there is a critical gap in the literature on neurodevelopmental trajectories from early to late childhood, making it difficult (1) to assess the effect of high ELA exposure on brain development and (2) to identify sensitive time windows for intervention during childhood.

Recent studies on neurodevelopmental trajectories have focused on the correlation between structural and functional connectivity, that is, structure–function coupling (SC–FC), as a measure to capture changes in brain organization and maturation. Between the ages of 8 and 22 years, SC–FC changes in a functional-network-specific manner, with decreases in highly conserved motor regions and increases in transmodal cortices[15]. In adults, SC–FC is highest in unimodal cortical regions and lowest in transmodal cortices[16]. Whereas high SC–FC implies functional communication supported directly by local white-matter pathways, low SC–FC suggests that functional communication relies on polysynaptic indirect pathways (circuit-level modulation) and a greater capacity for plasticity[15]. The extent of SC–FC is linked to behavioral outcomes, such as executive function and higher cognitive abilities[17–19]. Notably, significant SC–FC in the reward network is associated with poor performance on executive function tasks in later childhood[19]. Therefore, SC–FC captures information on age and the current state of plasticity (highly conserved unimodal regions versus transmodal regions with increased potential for plasticity)[16].

Current SC–FC studies focus on adolescents and adults, such that SC–FC trajectories have not been studied in children. Studies of ELA will predict outcomes apparent in early childhood, consistent with early biological embedding of experience. To examine this hypothesis, we leveraged data from the deeply phenotyped Growing Up in Singapore Towards healthy Outcomes (GUSTO) birth cohort (Table 1 and Extended Data Fig. 1) to investigate whether or not neurodevelopment, estimated by SC–FC averaged across the whole cortex, is accelerated in children exposed to high ELA. We focused on measures of prenatal adversity (Supplementary Section 1.1) based on previous neuroimaging studies showing associations with brain structure at birth[20–22] as well as analyses revealing the fetal neurodevelopment period as a time of peak expression of genes associated with a range of neuropsychiatric disorders[23]. Despite the evidence of prenatal adversity as a risk factor for psychopathology, it is still unclear how prenatal adversity influences the pace

Table 1 | Summary of demographics for the neuroimaging dataset and the dataset with complete neuroimaging and adversity scores data

	Dataset			P value
	Full MRI		**Adversity + MRI**	
	N=549		**N=354**	
Sex				0.73
Female	280	(51.0%)	176	(49.7%)	
Male	269	(49.0%)	178	(50.3%)	
Ethnicity				0.58
Chinese	295	(53.7%)	179	(50.6%)	
Indian	92	(16.8%)	56	(15.8%)	
Malay	161	(29.3%)	118	(33.3%)	
Other	1	(0.2%)	1	(0.3%)	
Gestational age (weeks)	38.8	(±1.4)	38.9	(±1.3)	0.64
Maternal age at birth (years)	31.1	(±5.2)	30.8	(±5.1)	0.33
Highest maternal education				0.28
None/primary	30	(5.5%)	19	(5.4%)	
Secondary/technical	218	(39.7%)	144	(40.7%)	
GCE 'A' levels/university	295	(53.7%)	191	(54.0%)	
Missing (NA)	6	(1.1%)	0	(0.0%)	
Household monthly income (SGD)				0.28
<2,000	80	(14.6%)	49	(13.8%)	
2,000–5,999	309	(56.3%)	211	(59.6%)	
≥6,000	124	(22.6%)	81	(22.9%)	
Missing (NA)	36	(6.6%)	13	(3.7%)	

Continuous variables are presented as the mean±s.d. (in parentheses). Two-sample *t*-tests were used to assess group differences for continuous variables. Fisher's exact test for proportions was used to assess group differences for categorical variables. The *P* values reported are two-tailed. MRI, Magnetic resonance imaging; NA, Not available; SGD, Singapore dollars.

of neurodevelopment in childhood. We first modeled SC–FC changes over three time points (ages of 4.5, 6 and 7.5 years) in our full neuroimaging cohort, which is a mixture of distinct and repeated samples (Fig. 1 and Supplementary Section 1.2). Our three time points correspond to two standard childhood phases—preschool and mid-childhood[24]. We then stratified our cohort via groups with exposure to different levels of adversity (no adversity, low adversity and high adversity) and compared the SC–FC trajectories between these groups. Next, we investigated whether or not the trajectory differences were specific to transmodal association regions with protracted development. We specifically examined the frontoparietal network (FPN) and the visual network (VIS), functional networks that represent transmodal regions and unimodal regions, respectively[25]. We hypothesized that accelerated development would be observed in the high-adversity group, which would be specific to transmodal association regions. Finally, we performed exploratory analyses studying whether or not SC–FC at our earliest time point (age 4.5 years) altered a child's susceptibility to developing psychopathologies, that is, it modulated the effects of adversity scores on behavioral outcomes in childhood.

Results
SC–FC trajectories over childhood and stratified by ELA
Resting-state functional MRI (rs-fMRI) and diffusion tensor imaging data from 549 participants (Table 1) were included in the current study, for a total of 917 scans over the three time points (age range, 4.4–8 years). For each participant, structural connectivity (indexed by
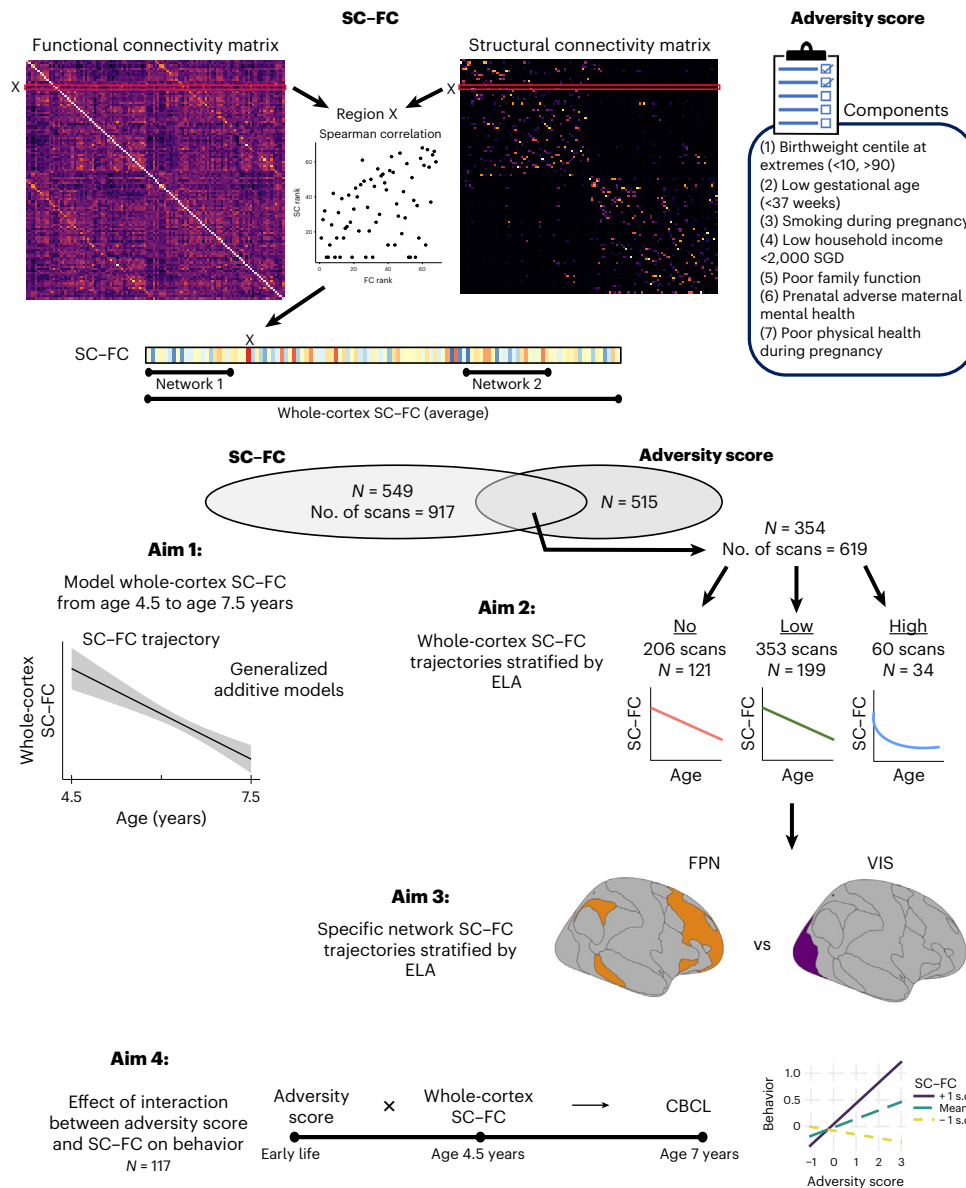
Fig. 1 | Study design and aims. Regional SC–FC values were calculated for a 114-region cortical parcellation through the Spearman correlation of structural connectivity (SC) and functional connectivity (FC) values of each region (colors are arbitrary and for qualitative purposes). Whole-cortex SC–FC was calculated by averaging values across all 114 regions. Network-specific coupling was calculated by averaging values across regions assigned to a network. Cumulative adversity scores were calculated based on seven components. This enabled us to model non-linear SC–FC trajectories (solid black line ± 95% confidence interval)

over three time points (age 4.5, 6 and 7.5 years; age range, 4.4–8 years), as well as stratified by exposure to adversity ('No' (no adversity), score 0, $N = 121$, total of 206 scans; 'Low' (low adversity), score 1–2, $N = 199$, total of 353 scans; 'High' (high adversity), score >3, $N = 34$, total of 60 scans). The Child Behavior Checklist (CBCL) was administered at age 7 years to detect internalizing and externalizing problems. Brain network images were made using the ggsegYeo2011 package[73] (https://doi.org/10.5281/zenodo.4896734).

streamline densities) and functional connectivity matrices were estimated for each pair of a 114-region cortical parcellation. Whole-cortex SC–FC was calculated by deriving the Spearman correlation between non-zero structural and functional connectivity values for each region, and taking the mean of all 114 regions. Whole-cortex SC–FC trajectories, modeled via generalized additive models (GAMs), decreased linearly from age 4.5 to 7.5 years (Fig. 2a; effective degrees of freedom (e.d.f.) = 1.006, $F = 114.9$, $P < 0.001$).

Prospective data collection of pregnancy and early-life measures were used to calculate the ELA exposure in a subset of participants ($N = 354$, total of 619 scans). When the cohort was stratified by ELA exposure (Fig. 2b,c), we observed a linear decrease in SC–FC averaged across the whole cortex for the no-adversity and low-adversity groups

($e.d.f. = 1$, $F > 30$, $P < 0.001$). A curvilinear decrease was observed only for the high-adversity group ($e.d.f. = 1.8$, $F = 9.6$, $P < 0.001$; Supplementary Section 2), suggesting that SC–FC decreased at a different rate between 4.5 and 6 and between 6 and 7.5 years of age.

To compare the trajectories, we plotted the difference curves for each pair of trajectories (Fig. 2d). The trajectories for the no-adversity and low-adversity groups were similar. The difference curves that compare the no- or low-adversity groups with the high-adversity group have similar shapes, with a negative value (a greater decrease for high adversity relative to low adversity) between ages 4.5 and 6 years, and a positive value (a lesser decrease for high adversity relative to low adversity) between ages 6 and 7.5 years. The greatest difference was observed between the low- and high-adversity trajectories.
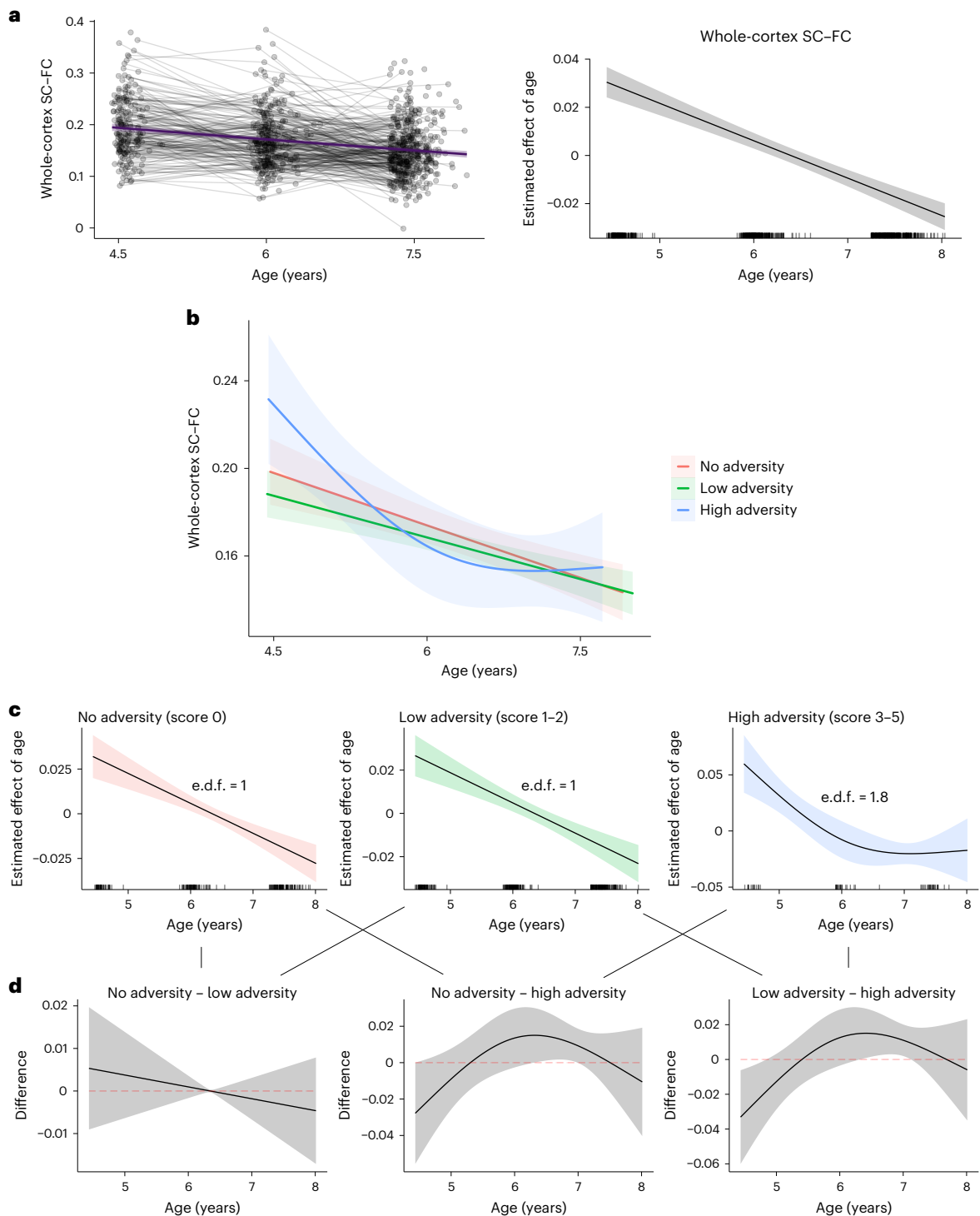
Fig. 2 | Modeling SC–FC trajectories with GAMs. a, In the left panel, SC–FC (*N* = 549, total of 917 scans) averaged across the whole cortex, modeled over age 4.5 to 7.5 years using GAMs, is shown as the mean estimate (purple line) ±95% confidence intervals (purple shading). Individual trajectories based on actual data across the three time points are plotted in black. The right panel displays the GAM-estimated additive effect of age (solid line ± shaded 95% confidence interval). Black markings on the x-axis show individual age data points. **b**, SC–FC trajectories stratified by ELA scores (*N* = 354, total of 619 scans; categorized as no adversity, low adversity and high adversity) displayed on the same scale. **c**,**d**, Trajectories estimating the effect of the time point displayed separately for each adversity group (**c**) and the difference curves graphically showing the differences between each pair of trajectories (**d**). Trajectories are considered to be significantly different if the confidence interval does not include zero (dashed red line). GAM results for **b**–**d** are displayed as the mean estimates (solid lines) ±95% confidence intervals (shaded areas).

Modeling using GAMS suggested that there was a greater decrease in SC–FC in the high-adversity group relative to the low-adversity group during early childhood. We tested this statistically using linear mixed effects (LME) models (ages 4.5 to 6; *N* = 251, total of 343 scans) and found that Adversity$_{Low}$:Age was significantly higher relative to Adversity$_{High}$:Age (Fig. 3a; estimate = 0.024, s.e.m. = 0.012, *t* = 2.05, *P* (one-tailed) = 0.022; Supplementary Section 3a) on SC–FC averaged across the whole cortex.
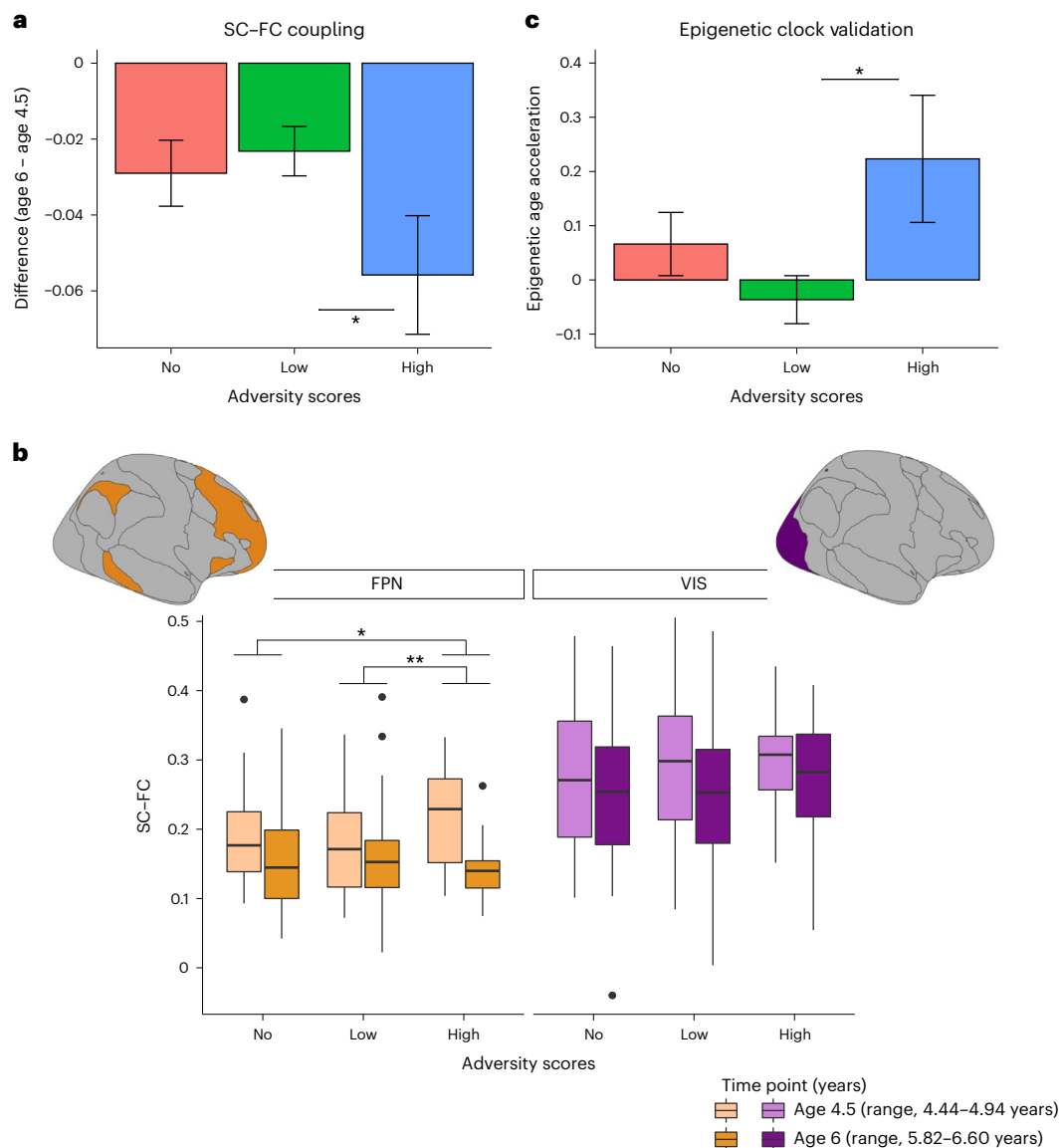
Fig. 3 | Model estimates from LME models. a,b, An accelerated decrease in SC–FC between ages 4.5 and 6 years in the high-adversity group (*N* = 25, total of 34 scans) relative to the low-adversity group (*N* = 143, total of 197 scans) was observed for the whole cortex (*P* = 0.022) (**a**) and for the FPN (*P* = 0.007) (**b**) but not for the VIS (*P* = 0.438) (**b**). Results were estimated using LME models, and one-tailed *P* values reported are for the Adversity_Low:Age interaction term. In **a**, the bar charts show model estimates of the mean ± s.e.m. In **b**, the boxplots are displayed as the Tukey's five number summary (the bold horizontal line denotes the median; the lower and upper hinges denote the first and third quartiles, respectively; the whiskers extend to the furthest data point within

1.5 × the interquartile range; and the dots exceeding the whiskers denote outliers). **c**, DNA methylation-based epigenetic age acceleration (*N* = 241) at age 6 years is significantly higher in the high-adversity group (*N* = 25) relative to the low-adversity group (*N* = 132; *P* = 0.01). The *P* values (one-tailed) reported were estimated using a linear regression model. Data in the bar charts show the mean ± s.e.m. of the actual data. No multiple comparison corrections were performed. For all plots, **P* < 0.05, ***P* < 0.01. The brain network images in **b** were made using the ggsegYeo2011 package[73] (https://doi.org/10.5281/zenodo.4896734).

We next explored whether or not this finding was different in specific functional networks (Fig. 3b). LME models were performed specifically for the VIS and the FPN, which represent a unimodal sensory network and a transmodal network that matures slowly, respectively. We found that Adversity_Low:Age was significantly higher relative to Adversity_High:Age for the FPN (estimate = 0.033, s.e.m. = 0.013, *t* = 2.51, *P* (one-tailed) = 0.007) but not for the VIS (estimate = 0.004, s.e.m. = 0.023, *t* = 0.16, *P* (one-tailed) = 0.44), suggesting a higher susceptibility of transmodal brain networks. To confirm this finding, we performed LME models (1) without covariates to obtain unadjusted estimates and (2) with potential confounders (Supplementary Section 3b). We also performed LME models for the remaining networks, and

observed a similar accelerated decrease for the default mode network (DMN) and salience network, both of which are transmodal networks (Supplementary Section 3c and Extended Data Fig. 2).

Validation

Epigenetic age. Given that SC–FC decreased over our time period of interest, the accelerated decrease between ages 4.5 and 6 years observed for the high-adversity group suggests accelerated neurodevelopment. To validate our finding, we assessed age acceleration at age 6 years based on DNA-derived methylation epigenetic clocks (*N* = 241). We found that age acceleration was significantly higher in the high-adversity group relative to the low-adversity group (Fig. 3c;
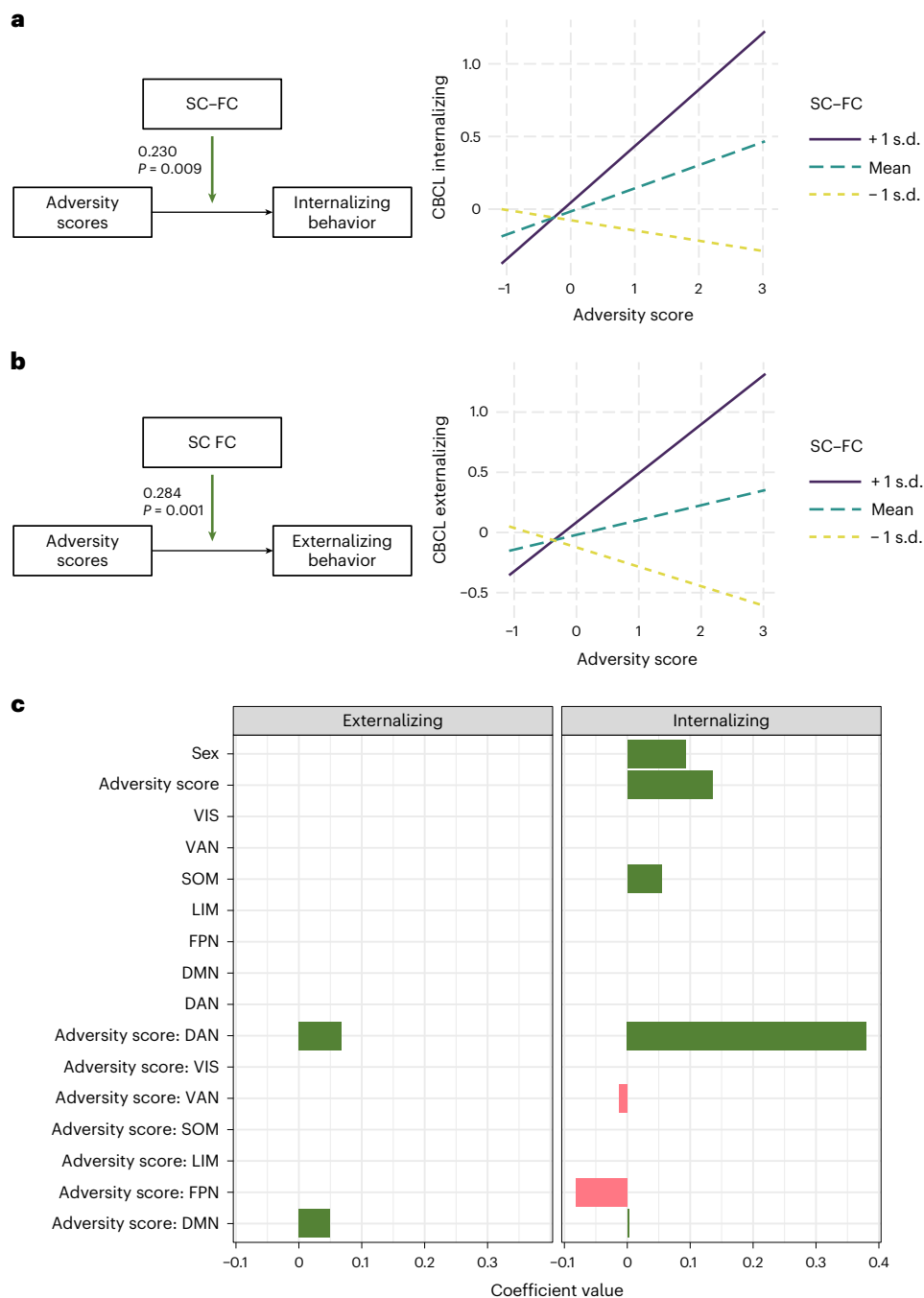
Fig. 4 | Adversity scores, whole-cortex SC–FC and the CBCL. a,b, A significant interaction between adversity scores and whole-cortex SC–FC (N = 117) was observed for internalizing behaviors (**a**) and externalizing behaviors (**b**) assessed by the CBCL. Model estimates were obtained from linear regression models. **c,** Summary of the coefficients of variables selected by the elastic net regression models. The direction of modulation, positive or negative, is displayed as green or red, respectively. VAN, ventral attention network; SOM, somatomotor network; LIM, limbic network.

estimate = 0.28, s.e.m. = 0.12, t = 2.36, P (one-tailed) = 0.0095). We observed a similar pattern to SC–FC where the greatest difference was found between the high- and low-adversity groups, whereas the low- and no-adversity groups were similar to each other.

Sensitivity analysis. We replicated our LME findings in a small independent dataset (30 scans) (Supplementary Section 4a). Given the confounding effects of motion on neuroimaging data, especially in young children, we performed sensitivity analyses on an extended dataset excluding subsets of scans based on different motion criteria.

The main findings remained unchanged (Supplementary Section 4b). SC–FC estimates were also assessed to be reliable for our quantity of available data (Supplementary Section 4c), and with strict motion parameters (Supplementary Section 4d).

Association with behavioral outcomes
The ELA scores were positively and significantly correlated with child behavioral problems at age 7 years (N = 427). High adversity scores were associated with an increased risk of both internalizing (Pearson's r = 0.22, P < 0.001) and externalizing behaviors (Pearson's r = 0.20, P < 0.001).

We then examined whether or not SC–FC would moderate the association of ELA scores with the CBCL at age 7 years ($N = 117$). We used SC–FC averaged across the whole cortex at age 4.5 years as the moderator variable. The interaction between SC–FC and adversity scores had a significant association with both internalizing (estimate = 0.23, s.e.m. = 0.086, $t = 2.66$, $P = 0.0089$) and externalizing behaviors (estimate = 0.28, s.e.m. = 0.086, $t = 3.31$, $P = 0.0013$). Simple slope analyses revealed that a significant positive correlation between adversity scores and externalizing/internalizing behavior was only present when SC–FC was high at age 4.5 years (Fig. 4a,b).

To explore network-specific modulation, we examined the interaction between SC–FC for seven functional networks and adversity scores. The dorsal attention network (DAN) interaction term is highlighted as having the highest estimated coefficient, suggesting a strong positive modulatory effect, especially on internalizing behavior (Fig. 4c).

Similarly, we found network-specific modulatory effects on relational aggression and frustration levels (Supplementary Section 5).

Discussion

Our study modeled SC–FC changes from preschool to mid-childhood. Thus, we address a critical gap in the neurodevelopmental literature, which previously lacked longitudinal neuroimaging data starting from the preschool age. The relevance of these data can be best appreciated when considering the importance of this period of neurodevelopment for a range of socioemotional and cognitive functions[26]. Our finding of an accelerated decrease in SC–FC for the high-adversity group between ages 4.5 and 6 years suggests this time period as a potential window for intervention to reduce the effects of ELA on later outcomes. In addition, our findings portray the heterogeneity in neurodevelopment over different stages of childhood and highlight the limitations of collapsing children into a single cohort.

We observed that SC–FC changes as a function of age during childhood—specifically, there is a positive association between structural connectivity and functional connectivity that weakens from age 4.5 to 7.5 years. This reflects the diverse processes underlying neurodevelopment that follow different timelines. From the neurodevelopmental literature, the brain undergoes pronounced yearly change during the preschool years[26]. White-matter tracts show increases in fiber density and bundle size, suggesting a gradual increase in structural connectivity[27]. By contrast, functional connectivity tends to follow a pattern of overconnectivity, followed by pruning and restructuring to achieve functional network segregation[28]. In addition, brain SC–FC is thought to be a measure of plasticity where high coupling implies high regional specialization/low plasticity[15]. During early childhood, low specialization and high plasticity are expected due to the ongoing neurodevelopmental processes. Our understanding of neurodevelopmental processes during early childhood matches the observed decrease in SC–FC. In sum, SC–FC is a promising summary measure for capturing changes in brain connectivity and organization during childhood that can be used to identify abnormalities in developmental trajectories.

We showed that exposure to prenatal adversity is associated with a steeper decrease in SC–FC between ages 4.5 and 6 years, suggesting accelerated development. However, we acknowledge that the steeper slope between 4.5 and 6 years observed in the high-adversity group may be due to the higher SC–FC at age 4.5 years, and could potentially represent 'catch up' development to the norm at age 7.5 years. Nevertheless, it is evident that the developmental trajectory of brain maturation in young children is altered as a result of ELA exposure. For instance, exposure to low socioeconomic status (SES) has been linked to changes in cortical thickness and functional segregation[5]. Cortical thickness peaks at around age 2 years, and exposure to low SES is associated with cortical thinning occurring earlier in life[29]. These findings are suggested to reflect an earlier curtailment of synaptic proliferation and a decreased window for synaptic pruning. Other studies suggest that higher SES is linked to more protracted functional network

development[30,31]. Tooley et al. suggest a theoretical model where the extended period of structural development associated with high SES is reflected in functional segregation, that is, a slower trajectory of functional network segregation[5]. Our findings suggest that whereas accelerated development is sufficiently widespread to be detected by averaging over the whole cortex, regions with a longer maturation window are particularly susceptible. Indistinct cortical boundaries of transmodal association networks[32] support the hypothesis that these brain networks undergo protracted development and are more susceptible to factors influencing development. Lin et al. postulate that protracted development enables adaptive developmental plasticity in behaviors such as learning[33]. This understanding suggests that accelerated development occurs in networks such as the FPN and DMN because these regions are important for experience-dependent learning. Our study adds to this literature by showing that accelerated development in the form of a reduced window for neural plasticity—as captured by a steeper SC–FC decrease—in transmodal regions with protracted development may occur during early childhood as a result of exposure to prenatal adversity. This is not surprising as substantial brain development occurs in utero. Moreover, exposure to prenatal adversity is postulated to increase susceptibility to postnatal influences[2], highlighting the distinct complementary effects of prenatal and postnatal adversity on neurodevelopment.

The literature on prenatal stress suggests several mechanisms through which the in utero environment could affect downstream development. These include alterations in the neuroendocrine and immune system that have a sustained impact on later life development[34]. Glucocorticoids and pro-inflammatory cytokines have widespread effects in the brain and have been considered as candidate mechanisms for the effects of prenatal stress on child outcomes[35–37]. These chemical messengers act as signals that influence cell-signaling pathways (for example, regulating enzyme activity), which in turn influence neurotransmission and the proper formation of neural circuits and maintenance.

Contrary to previous literature using the ACE framework, we did not observe a graded response between our three groups. One possibility is that our adversity score was computed with population-based measures (for example, SES or birth weight) as opposed to the typical ACE questionnaire which focuses on childhood maltreatment[38]. Our adversity score did not include any categories of abuse. Thus, the literature on neglect/poverty and developmental support, which are also highly predictive of child developmental outcomes[39], may be more relevant to our study. In addition, Keding et al. show that physical neglect is linked to widespread accelerated maturation, although exposure to abuse in girls is associated with delayed maturation in emotion circuitry[40]. Although we observed the greatest differences between the low- and high-adversity groups, we did not observe any differences between the no- and low-adversity groups. When we combined the no-adversity and low-adversity groups, we obtained the same results—accelerated decrease between ages 4.5 and 6 years in the high-adversity group relative to the low-adversity group (Supplementary Section 6).

Results from our exploratory analyses showed that a positive association between prenatal adversity scores and both internalizing and externalizing behaviors was only observed for high SC–FC at age 4.5 years. Follow-up analysis suggests that the DAN plays a role in modulating the effect of ELA on externalizing and internalizing behaviors. Herzberg et al. also show circuit-specific adaptations following early-life stress—within-DAN functional connectivity differed between previously institutionalized youths and controls, and was positively associated with both internalizing and externalizing symptoms[41]. The DAN may also be important for recovery processes after stress exposure, a potential mechanism through which later life behavior is affected[42]. We also found positive whole-cortex and network-specific modulatory effects with a child-report measure of relational aggression

and a task-based measure of emotion regulation (Supplementary Section 5). It may be worthwhile to explore network-specific SC–FC in relation to different dimensions of psychopathologies in future studies.

Some limitations should be considered when interpreting the study findings. First, as our study population is largely a typically developing cohort, the sample size for the high-adversity group was small relative to the low/no-adversity groups. This feature may increase the risk of overfitting curves and limits our ability to stratify further the population by sex, even though sex was a significant covariate in our analyses (Supplementary Section 3a). Our findings also suggest that the associations between adversity and behavioral problems are different at different degrees of SC–FC, but may be under-powered to detect a mediation effect. Second, motion is always a possible confounder for neuroimaging studies, and collecting high-quality neuroimaging data is especially challenging in pediatric populations under age 7 years. We corrected for motion during pre-processing, and also conducted a sensitivity analysis based on motion criteria, and the main findings remain unchanged. Moreover, a relatively short rs-fMRI sequence (~5.32 min) was used to reduce the burden on young participants. However, the acquisition time of ~5½ min has been shown to produce stable functional connectivity estimates in children[43], as well as stable SC–FC estimates in our study (Supplementary Section 4c). Third, our study lacks imaging data before age 4.5 years; thus we were unable to establish the SC–FC developmental trajectory before age 4.5 years and can only interpret SC–FC changes between the ages of 4.5 and 7.5 years. As our dataset is semi-longitudinal, our trajectory estimates are at the group, not individual, level. Fourth, we focused on prenatal exposures of adversity, but results could potentially be correlated with postnatal adversity. Therefore, our findings do not necessarily inform on the timing of effects. Finally, our study data represent a Singaporean population, and replication in other cohorts is needed to assess the generalizability of our findings.

We present evidence that accelerated neurodevelopment occurs in regions with protracted development after exposure to ELA. This observation is probably an adaptive response to adjust to a suboptimal environment that results in a shortened window for plasticity-related learning. Our findings suggest that the period before the age of 6 years is critical, and they highlight the importance of early detection and intervention to ameliorate the effects of ELA on later life outcomes.

Methods

Methods are described in detail in Supplementary Section 1.

Subjects

Participants were part of the GUSTO study[44,45], a longitudinal, Singaporean community-based birth cohort. Neuroimaging data from 549 participants were included, with a total of 917 scans at ages of 4.5, 6 and 7.5 years. A subset of participants ($N = 354$) had sufficient data for adversity score computation (Table 1). The GUSTO study was approved by the National Healthcare Group Domain Specific Review Board (D/2009/021 and B/2014/00411) and the SingHealth Centralized Institutional Review Board (D/2018/2767 and A/2019/2406). All investigations were conducted according to the principles expressed in the Declaration of Helsinki. Written informed consent was obtained from all guardians on behalf of the children enrolled in this study. Participants received 150 SGD for each MRI session and an additional 120 SGD for questionnaires and laboratory-based tasks. The study followed the STROBE (strengthening the reporting of observational studies in epidemiology) reporting guidelines for cohort studies[46].

Adversity score calculation

Adversity scores focused on prenatal exposures and were calculated as described previously[47]. Adversity scores were based on seven components, and participants scored 1 point for each component if the respective criteria were met, resulting in a maximum score of 7 (Supplementary Section 1.1). On the basis of the ACE literature on cumulative adversity exposure, scores were re-categorized into three groups: no adversity (score 0, 33%), low adversity (score 1–2, 57%) and high adversity (>3, 10%) (Supplementary Section 1.1d).

MRI acquisition and pre-processing

Neuroimaging data were acquired at two sites using 3 T MRI scanners (Siemens). For each subject, diffusion-weighted, rs-fMRI and T_1-weighted images were collected.

Diffusion data were processed in FMRIB's Software Library (FSL v.6.0.4)[48]. A brain mask was created from the $b0$ image, underwent motion correction using the eddy tool (with an outlier threshold of 3 s.d.) and was de-noised using a local principal component analysis method[49]. The rs-fMRI data were processed with the default pre-processing and de-noising pipelines using the functional connectivity toolbox Conn (v.20b)[50] as described previously[19] (Supplementary Section 1.2).

Regions of interest and connectivity matrices

The regions of interest (ROIs) were 114 cortical regions[51] that were assigned to the seven functional networks identified by Yeo and co-workers[52]. For each scan, functional connectivity matrices were computed by measuring the bivariate correlation coefficients of the BOLD (blood oxygenation level-dependent) time series between each seed and target ROIs through a hemodynamic response factor-weighted general linear model. Structural connectivity matrices were computed by calculating streamline densities between each seed and target ROIs derived from probabilistic tractography using FSL's BEDPOSTX and PROBTRACKX tools[53,54].

Deriving structure–function coupling

The SC–FC was calculated as described in Baum et al.[15], where the Spearman correlation between non-zero structural and functional connectivity values was obtained for each region. Whole-cortex SC–FC was calculated by averaging values across all 114 regions. Network-specific coupling was calculated by averaging values across regions assigned to a network. As the first two time points (that is, ages 4.5 and 6 years) were collected at site 1, while the age 7.5 years data were collected at site 2, each region was harmonized across site using longitudinal ComBat (v.0.0.0.90)[55] (Supplementary Section 7).

Epigenetic clock

Epigenetic age was used as a validation measure of development. Blood was collected from participants at age 6 years, and was processed to obtain the buffy coat layer for DNA extraction. DNA methylation was profiled using an Infinium MethylationEPIC BeadChip array following the standard protocol[14]. Wu's epigenetic clock[56–58] and age acceleration (adjusted for cell counts, ageAcc3) were computed using the DNAmAge function from the methylclock package (v.0.99.25)[59]. The Wu clock was chosen as it was trained on both pediatric data and blood samples.

Child behavior outcomes

The Child Behavior Checklist (CBCL)[60] is used to detect behavioral and emotional problems in children. The CBCL was administered at age 7 years, and is a maternal-reported questionnaire that categorizes 118 items into internalizing and externalizing behaviors[61]. The CBCL subscales showed very good reliability in our cohort (Cronbach's $\alpha = 0.855$ for the internalizing subscale; Cronbach's $\alpha = 0.888$ for the externalizing subscale). Additional dimensions of psychopathology in relation to ELA are described in Supplementary Section 5.

Statistical analysis

All statistical analyses were performed in R (v.4.04)[62]. Sex was included as a covariate for all models. The alpha level was set at $P < 0.05$ (two-tailed unless stated otherwise).

Trajectory analysis. GAMs were used to model whole-cortex SC–FC (outcome) over the three time points (age range, 4.4–8.0 years) using the mgcv package (v.1.8-39)[63]. To model possible non-linear trajectories, a smoothing function f was applied to the age (predictor), where the e.d.f. statistic reflects the degree of non-linearity of a curve[64]. To account for longitudinal data, we also included a smoothing function f, equivalent to adding a random effect, for each subject[65]:

$$SC-FC = f(age) + f(subject) + sex + \in .$$

To model the SC–FC trajectories stratified by adversity groups, a second GAM was run with individual trajectories estimated for each adversity group:

$$SC-FC = adversity + f(age, by = adversity) + f(subject) + sex + \in .$$

Comparing adversity trajectories. Adversity trajectories were compared visually with difference curves and statistically with LME models. Difference curves were computed using the gratia package (v.0.7.2)[66] to assess differences between each pair of adversity trajectories (for example, no adversity minus low adversity). Trajectories are significantly different if the confidence interval of the difference curve does not include zero.

LME models were performed with the nlme package (v.3.1-160) and were used to assess whether or not the change in SC–FC between ages 4.5 and 6 years differed significantly between adversity groups (reference: high adversity), that is, a significant interaction between the adversity group and the time point[67]. Given our hypothesis of accelerated development, one-tailed *P* values were reported for interaction terms.

Validation of accelerated development. Regression analysis was used to compare whether or not epigenetic age acceleration was significantly different between the adversity groups, with high adversity as the reference group. The first three principle components of the genotyped autosomal single nucleotide polymorphisms were used as co-variates to adjust for population stratification as typically performed in analyses involving genetic datasets[68].

Associations with behavioral outcomes. Regression models were used to explore whether or not whole-cortex SC–FC modulated the effects of adversity scores on behavioral outcomes. Separate models were run for each measure. Simple slope analyses were conducted using the interactions package (v.1.1.5)[69] to analyse the post-hoc differences if the interaction was significant. Elastic net regression was performed, using the caret (v6.0-92) and glmnet (v4.1-2) packages[70,71], to explore network-specific modulators of behavioral outcomes. Predictors included adversity scores, seven functional-network-specific SC–FC measures and seven interaction terms (adversity scores × network-specific SC–FC).

Power analysis. The current study is part of an ongoing birth cohort; study objectives are not a primary outcome of the original cohort recruitment. Furthermore, given the longitudinal follow-up involved, the data in our study (especially the first time point of age 4.5 years) were collected several years before our study conception. Therefore, a power analysis was not conducted for this study as it has been suggested that post-hoc power analyses may not be very informative[72].

Reporting summary

Further information on research design is available in the Nature Portfolio Reporting Summary linked to this article.

Data availability

The GUSTO data are not deposited into a public repository due to multi-site partnership agreements and conditions for Internal Review Board approval. GUSTO data are routinely made available through submission and approval from the cohort executive committee of a data access form. Details may be obtained from the corresponding author upon reasonable request.

Code availability

No new algorithms were written for this study. Study analyses were carried out in R using published R packages. The R code is available from the corresponding author upon reasonable request.

References

1. Nelson, C. A. et al. Adversity in childhood is linked to mental and physical health throughout life. *Br. Med. J.* **371**, m3048 (2020).
2. O'Donnell, K. J. & Meaney, M. J. Fetal origins of mental health: the developmental origins of health and disease hypothesis. *Am. J. Psychiatry* **174**, 319–328 (2017).
3. Kee, M. Z. L. et al. Preconception origins of perinatal maternal mental health. *Arch. Womens Ment. Health* **24**, 605–618 (2021).
4. Teicher, M. H. & Samson, J. A. Annual research review: enduring neurobiological effects of childhood abuse and neglect. *J. Child Psychol. Psychiatry* **57**, 241–266 (2016).
5. Tooley, U. A., Bassett, D. S. & Mackey, A. P. Environmental influences on the pace of brain development. *Nat. Rev. Neurosci.* **22**, 372–384 (2021).
6. Snell-Rood, E. & Snell-Rood, C. The developmental support hypothesis: adaptive plasticity in neural development in response to cues of social support. *Philos. Trans. R. Soc. Lond. B Biol. Sci.* **375**, 20190491 (2020).
7. Callaghan, B. L. & Tottenham, N. The stress acceleration hypothesis: effects of early-life adversity on emotion circuits and behavior. *Curr. Opin. Behav. Sci.* **7**, 76–81 (2016).
8. Cowan, C. S., Callaghan, B. L. & Richardson, R. Acute early-life stress results in premature emergence of adult-like fear retention and extinction relapse in infant rats. *Behav. Neurosci.* **127**, 703–711 (2013).
9. Moriceau, S., Shionoya, K., Jakubs, K. & Sullivan, R. M. Early-life stress disrupts attachment learning: the role of amygdala corticosterone, locus ceruleus corticotropin releasing hormone, and olfactory bulb norepinephrine. *J. Neurosci.* **29**, 15745–15755 (2009).
10. Tottenham, N. et al. Prolonged institutional rearing is associated with atypically large amygdala volume and difficulties in emotion regulation. *Dev. Sci.* **13**, 46–61 (2010).
11. Gee, D. G. et al. Early developmental emergence of human amygdala–prefrontal connectivity after maternal deprivation. *Proc. Natl Acad. Sci. USA* **110**, 15638–15643 (2013).
12. Qiu, A. et al. Prenatal maternal depression alters amygdala functional connectivity in 6-month-old infants. *Transl. Psychiatry* **5**, e508–e508 (2015).
13. Sun, Y., Fang, J., Wan, Y., Su, P. & Tao, F. Association of early-life adversity with measures of accelerated bbiological aging among children in China. *JAMA Netw. Open* **3**, e2013588 (2020).
14. McGill, M. G. et al. Maternal prenatal anxiety and the fetal origins of epigenetic aging. *Biol. Psychiatry* **91**, 303–312 (2022).
15. Baum, G. L. et al. Development of structure–function coupling in human brain networks during youth. *Proc. Natl Acad. Sci. USA* **117**, 771–778 (2020).
16. Valk, S. L. et al. Genetic and phylogenetic uncoupling of structure and function in human transmodal cortex. *Nat. Commun.* **13**, 2341 (2022).
17. Reijmer, Y. D. et al. Decoupling of structural and functional brain connectivity in older adults with white matter hyperintensities. *Neuroimage* **117**, 222–229 (2015).
18. Wang, J. et al. Alterations in brain network topology and structural–functional connectome coupling relate to cognitive impairment. *Front. Aging Neurosci.* **10**, 404 (2018).

19. Chan, S. Y. et al. Structure–function coupling within the reward network in preschool children predicts executive functioning in later childhood. *Dev. Cogn. Neurosci.* **55**, 101107 (2022).

20. Rifkin-Graboi, A. et al. Prenatal maternal depression associates with microstructure of right amygdala in neonates at birth. *Biol. Psychiatry* **74**, 837–844 (2013).

21. Triplett, R. L. et al. Association of prenatal exposure to early-life adversity with neonatal brain volumes at birth. *JAMA Netw. Open* **5**, e227045 (2022).

22. Lee, A. et al. Long-term influences of prenatal maternal depressive symptoms on the amygdala–prefrontal circuitry of the offspring from birth to early childhood. *Biol. Psychiatry Cogn. Neurosci. Neuroimaging* **4**, 940–947 (2019).

23. Li, M. et al. Integrative functional genomic analysis of human brain development and neuropsychiatric risks. *Science* **362**, eaat7615 (2018).

24. Andersen, S. H. Association of youth age at exposure to household dysfunction with outcomes in early adulthood. *JAMA Netw. Open* **4**, e2032769 (2021).

25. Braga, R. M. & Leech, R. Echoes of the brain: local-scale representation of whole-brain functional networks within transmodal cortex. *Neuroscientist* **21**, 540–551 (2015).

26. Brown, T. T. & Jernigan, T. L. Brain development during the preschool years. *Neuropsychol. Rev.* **22**, 313–333 (2012).

27. Dimond, D. et al. Early childhood development of white matter fiber density and morphology. *Neuroimage* **210**, 116552 (2020).

28. Menon, V. Developmental pathways to functional brain networks: emerging principles. *Trends Cogn. Sci.* **17**, 627–640 (2013).

29. Piccolo, L. R., Merz, E. C., He, X., Sowell, E. R. & Noble, K. G. Age-related differences in cortical thickness vary by socioeconomic status. *PLoS ONE* **11**, e0162511 (2016).

30. Tooley, U. A. et al. Associations between neighborhood SES and functional brain network development. *Cereb. Cortex* **30**, 1–19 (2020).

31. Gellci, K. et al. Community and household-level socioeconomic disadvantage and functional organization of the salience and emotion network in children and adolescents. *Neuroimage* **184**, 729–740 (2019).

32. Tooley, U. A., Bassett, D. S. & Mackey, A. P. Functional brain network community structure in childhood: unfinished territories and fuzzy boundaries. *Neuroimage* **247**, 118843 (2022).

33. Lin, W. C., Delevich, K. & Wilbrecht, L. A role for adaptive developmental plasticity in learning and decision making. *Curr. Opin. Behav. Sci.* **36**, 48–54 (2020).

34. Roubinov, D., Meaney, M. J. & Boyce, W. T. Change of pace: how developmental tempo varies to accommodate failed provision of early needs. *Neurosci. Biobehav. Rev.* **131**, 120–134 (2021).

35. Hantsoo, L., Kornfield, S., Anguera, M. C. & Epperson, C. N. Inflammation: a proposed intermediary between maternal stress and offspring neuropsychiatric risk. *Biol. Psychiatry* **85**, 97–106 (2019).

36. Rudolph, M. D. et al. Maternal IL-6 during pregnancy can be estimated from newborn brain connectivity and predicts future working memory in offspring. *Nat. Neurosci.* **21**, 765–772 (2018).

37. Hall, B. S., Moda, R. N. & Liston, C. Glucocorticoid mechanisms of functional connectivity changes in stress-related neuropsychiatric disorders. *Neurobiol. Stress* **1**, 174–183 (2015).

38. Felitti, V. J. et al. Relationship of childhood abuse and household dysfunction to many of the leading causes of death in adults. The adverse childhood experiences (ACE) study. *Am. J. Prev. Med.* **14**, 245–258 (1998).

39. Luby, J. et al. The effects of poverty on childhood brain development: the mediating effect of caregiving and stressful life events. *JAMA Pediatr.* **167**, 1135–1142 (2013).

40. Keding, T. J. et al. Differential patterns of delayed emotion circuit maturation in abused girls with and without internalizing psychopathology. *Am. J. Psychiatry* **178**, 1026–1036 (2021).

41. Herzberg, M. P. et al. Accelerated maturation in functional connectivity following early life stress: circuit specific or broadly distributed? *Dev. Cogn. Neurosci.* **48**, 100922 (2021).

42. Broeders, T. A. A. et al. Dorsal attention network centrality increases during recovery from acute stress exposure. *NeuroImage Clin.* **31**, 102721 (2021).

43. White, T. et al. Time of acquisition and network stability in pediatric resting-state functional magnetic resonance imaging. *Brain Connect.* **4**, 417–427 (2014).

44. Soh, S. E. et al. Insights from the growing up in Singapore towards healthy outcomes (GUSTO) cohort study. *Ann. Nutr. Metab.* **64**, 218–225 (2014).

45. Soh, S. E. et al. Cohort profile: growing up in Singapore towards healthy outcomes (GUSTO) birth cohort study. *Int. J. Epidemiol.* **43**, 1401–1409 (2014).

46. von Elm, E. et al. Strengthening the reporting of observational studies in epidemiology (STROBE) statement: guidelines for reporting observational studies. *Br. Med. J.* **335**, 806–808 (2007).

47. Silveira, P. P. et al. Cumulative prenatal exposure to adversity reveals associations with a broad range of neurodevelopmental outcomes that are moderated by a novel, biologically informed polygenetic score based on the serotonin transporter solute carrier family C6, member 4 (*SLC6A4*) gene expression. *Dev. Psychopathol.* **29**, 1601–1617 (2017).

48. Smith, S. M. et al. Advances in functional and structural MR image analysis and implementation as FSL. *Neuroimage* **23**, S208–S219 (2004).

49. Manjón, J. V. et al. Diffusion weighted image denoising using overcomplete local PCA. *PLoS ONE* **8**, e73021 (2013).

50. Whitfield-Gabrieli, S. & Nieto-Castanon, A. Conn: a functional connectivity toolbox for correlated and anticorrelated brain networks. *Brain Connect.* **2**, 125–141 (2012).

51. Yeo, B. T., Tandi, J. & Chee, M. W. Functional connectivity during rested wakefulness predicts vulnerability to sleep deprivation. *Neuroimage* **111**, 147–158 (2015).

52. Yeo, B. T. et al. The organization of the human cerebral cortex estimated by intrinsic functional connectivity. *J. Neurophysiol.* **106**, 1125–1165 (2011).

53. Behrens, T. E., Berg, H. J., Jbabdi, S., Rushworth, M. F. & Woolrich, M. W. Probabilistic diffusion tractography with multiple fibre orientations: what can we gain? *Neuroimage* **34**, 144–155 (2007).

54. Behrens, T. E. et al. Characterization and propagation of uncertainty in diffusion-weighted MR imaging. *Magn. Reson. Med.* **50**, 1077–1088 (2003).

55. Beer, J. C. et al. Longitudinal ComBat: a method for harmonizing longitudinal multi-scanner imaging data. *Neuroimage* **220**, 117129 (2020).

56. Wu, X. et al. DNA methylation profile is a quantitative measure of biological aging in children. *Aging (Albany NY)* **11**, 10031–10051 (2019).

57. Kling, T., Wenger, A. & Carén, H. DNA methylation-based age estimation in pediatric healthy tissues and brain tumors. *Aging (Albany NY)* **12**, 21037–21056 (2020).

58. Wang, J. & Zhou, W. H. Epigenetic clocks in the pediatric population: when and why they tick? *Chin. Med. J. (Engl.)* **134**, 2901–2910 (2021).

59. Pelegí-Sisó, D., de Prado, P., Ronkainen, J., Bustamante, M. & González, J. R. *methylclock*: a Bioconductor package to estimate DNA methylation age. *Bioinformatics* **37**, 1759–1760 (2021).

60. Achenbach, T. M. & Rescorla, L. A. *Manual for the ASEBA School-Age Forms & Profiles* (ASEBA, 2001).

61. Achenbach, T. M. International findings with the Achenbach System of Empirically Based Assessment (ASEBA): applications to clinical services, research, and training. *Child Adolesc. Psychiatry Ment. Health* **13**, 30 (2019).

62. R Core Team, *R: a language and environment for statistical computing* (R Foundation for Statistical Computing, 2021).

63. Wood, S. N. Fast stable restricted maximum likelihood and marginal likelihood estimation of semiparametric generalized linear models. *J. R. Stat. Soc. Ser. B Stat. Methodol.* **73**, 3–36 (2011).

64. Wood, S. N. *Generalized Additive Models: An Introduction with R, 2nd Edition* (Chapman and Hall/CRC, 2017).

65. Mundo, A. I., Muldoon, T. J. & Tipton, J. R. Generalized additive models to analyze non-linear trends in biomedical longitudinal data using R: beyond repeated measures ANOVA and linear mixed models. *Stat Med.* **20**, 4266–4283 (2022).

66. Simpson, G. gratia: Graceful ggplot-Based Graphics and Other Functions for GAMs Fitted using mgcv. R package v.0.7.3 (2022).

67. Pinheiro J, Bates D, R Core Team (2023). nlme: Linear and Nonlinear Mixed Effects Models. R package version3.1-163, https://CRAN.R-project.org/package=nlme.

68. Patterson, N., Price, A. L. & Reich, D. Population structure and eigenanalysis. *PLoS Genet.* **2**, e190 (2006).

69. Long, J.A. interactions: Comprehensive, User-Friendly Toolkit for Probing Interactions. R package v.1.1.0 (2019).

70. Friedman, J., Hastie, T. & Tibshirani, R. Regularization paths for generalized linear models via coordinate descent. *J. Stat. Softw.* **33**, 1–22 (2010).

71. Kuhn, M. Building predictive models in R using the caret package. *J. Stat. Softw.* **28**, 1–26 (2008).

72. Yiran, Z. et al. Post hoc power analysis: is it an informative and meaningful analysis? *Gen. Psychiatry* **32**, e100069 (2019).

73. Mowinckel, A. M. ggseg/ggsegYeo2011. *Zenodo* https://doi.org/10.5281/zenodo.4896734 (2021).

Author contributions

Conceptualization was done by S.Y.C. and A.P.T. Data processing was carried out by S.Y.C., Z.M.N., Z.Y.O., J.L.M. and A.L.T. Formal analysis and manuscript preparation was performed by S.Y.C. Review and editing was carried out by M.Z.L.K., J.H.Z., M.S.K., P.P.S., A.P.T. and M.J.M. Supervision was provided by M.J.M. and A.P.T. Project administration and funding acquisition were provided by M.V.F., F.Y. and M.J.M.

Competing interests

The authors declare no competing interests.

Additional information

Supplementary information The online version contains supplementary material available at https://doi.org/10.1038/s44220-023-00162-5.

Correspondence and requests for materials should be addressed to Shi Yu Chan or Ai Peng Tan.
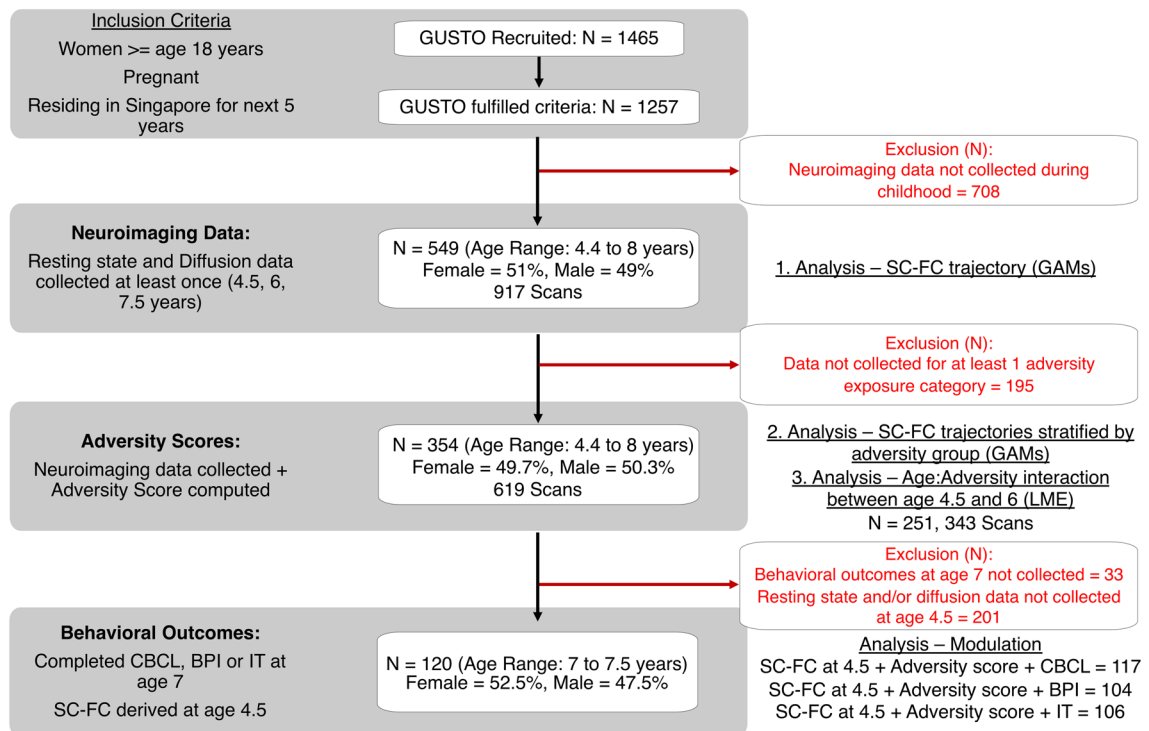
Peer review information *Nature Mental Health* thanks the anonymous reviewers for their contribution to the peer review of this work.

Reprints and permissions information is available at www.nature.com/reprints.

Publisher's note Springer Nature remains neutral with regard to jurisdictional claims in published maps and institutional affiliations.
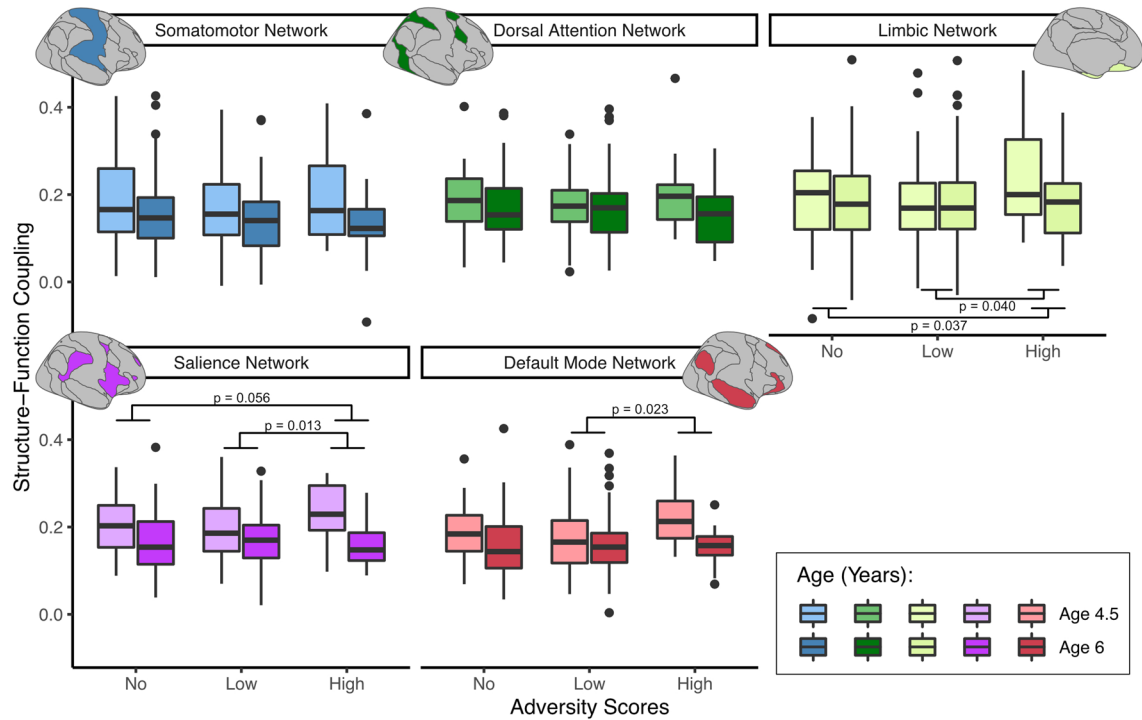
Inclusion Criteria

Women >= age 18 years

Pregnant

Residing in Singapore for next 5 years

GUSTO Recruited: N = 1465

GUSTO fulfilled criteria: N = 1257

Exclusion (N):
Neuroimaging data not collected during childhood = 708

Neuroimaging Data:

Resting state and Diffusion data collected at least once (4.5, 6, 7.5 years)

N = 549 (Age Range: 4.4 to 8 years)
Female = 51%, Male = 49%
917 Scans

1. Analysis – SC-FC trajectory (GAMs)

Exclusion (N):
Data not collected for at least 1 adversity exposure category = 195

Adversity Scores:

Neuroimaging data collected + Adversity Score computed

N = 354 (Age Range: 4.4 to 8 years)
Female = 49.7%, Male = 50.3%
619 Scans

2. Analysis – SC-FC trajectories stratified by adversity group (GAMs)
3. Analysis – Age:Adversity interaction between age 4.5 and 6 (LME)
N = 251, 343 Scans

Exclusion (N):
Behavioral outcomes at age 7 not collected = 33
Resting state and/or diffusion data not collected at age 4.5 = 201

Behavioral Outcomes:

Completed CBCL, BPI or IT at age 7

SC-FC derived at age 4.5

N = 120 (Age Range: 7 to 7.5 years)
Female = 52.5%, Male = 47.5%

Analysis – Modulation
SC-FC at 4.5 + Adversity score + CBCL = 117
SC-FC at 4.5 + Adversity score + BPI = 104
SC-FC at 4.5 + Adversity score + IT = 106

Extended Data Fig. 1 | Study Flowchart. The GUSTO cohort involves multiple waves of data collection from mother-child dyads. Pregnant women were recruited during their first trimester, during which demographic and maternal measures were collected. Neuroimaging data was collected at three study time-points during childhood (age 4.5, 6, 7.5 years) – participants were included if they had data collected at at least one time-point. Finally, child behaviour data was assessed at age 7 years. Sample size for each analysis was based on complete available data at that stage. Note: SC-FC, Structure-function coupling; GAM, Generalized Additive Model; LME, Linear Mixed Effects model; CBCL, Child Behavior Checklist; BPI, Berkeley Puppet Interview; IT, Impossible Tangram.

Extended Data Fig. 2 | Network-specific SC-FC between age 4.5 and 6 for remaining networks. Accelerated decrease in SC-FC between age 4.5 and 6 in the high adversity group (N = 25, total of 34 scans) relative to low adversity group (N = 143, total of 197 scans) was observed for the Default Mode Network, Salience Network, and the Limbic Network. Results were estimated by LME models and p-values reported are one-tailed. Boxplots are displayed as Tukey's five number summary (the bold horizontal line denotes the median; lower and upper hinges denote the first and third quartiles, respectively; whiskers extend to the furthest data point within 1.5*IQR; dots exceeding whiskers denote outliers). Brain network images were made using the ggsegYeo2011 package[73] (https://doi.org/10.5281/zenodo.4896734).

Corresponding author(s): Ai Peng Tan

Last updated by author(s): Oct 6, 2023

Reporting Summary

Nature Portfolio wishes to improve the reproducibility of the work that we publish. This form provides structure for consistency and transparency in reporting. For further information on Nature Portfolio policies, see our Editorial Policies and the Editorial Policy Checklist.

Statistics

For all statistical analyses, confirm that the following items are present in the figure legend, table legend, main text, or Methods section.

n/a	Confirmed	
☐	☒	The exact sample size (*n*) for each experimental group/condition, given as a discrete number and unit of measurement
☐	☒	A statement on whether measurements were taken from distinct samples or whether the same sample was measured repeatedly
☐	☒	The statistical test(s) used AND whether they are one- or two-sided *Only common tests should be described solely by name; describe more complex techniques in the Methods section.*
☐	☒	A description of all covariates tested
☒	☐	A description of any assumptions or corrections, such as tests of normality and adjustment for multiple comparisons
☐	☒	A full description of the statistical parameters including central tendency (e.g. means) or other basic estimates (e.g. regression coefficient) AND variation (e.g. standard deviation) or associated estimates of uncertainty (e.g. confidence intervals)
☐	☒	For null hypothesis testing, the test statistic (e.g. *F*, *t*, *r*) with confidence intervals, effect sizes, degrees of freedom and *P* value noted *Give P values as exact values whenever suitable.*
☒	☐	For Bayesian analysis, information on the choice of priors and Markov chain Monte Carlo settings
☒	☐	For hierarchical and complex designs, identification of the appropriate level for tests and full reporting of outcomes
☐	☒	Estimates of effect sizes (e.g. Cohen's *d*, Pearson's *r*), indicating how they were calculated

Our web collection on statistics for biologists contains articles on many of the points above.

Software and code

Policy information about availability of computer code

Data collection	Neuroimaging data was processed with established pipelines - the CONN toolbox v20b (dependencies: SPM12) and the FMRIB Software Library (FSL) v6.0.4 (tools: Brain Extraction Tool [bet], TOPUP, eddy, eddy_quad, BEDPOSTX, PROBTRACKX, flirt, fnirt) T1 images were processed using the FreeSurfer cortical reconstruction pipeline v6: recon-all
Data analysis	Analysis was performed in R v4.04. R packages used are: mgcv v1.8-39; gratia v0.7.2; nlme v3.1-160; interactions v1.1.5; caret v6.0-92; glmnet v4.1-2; methylclock v0.99.25; longCombat v0.0.0.90; ggsegYeo2011 v1.0.2.002

For manuscripts utilizing custom algorithms or software that are central to the research but not yet described in published literature, software must be made available to editors and reviewers. We strongly encourage code deposition in a community repository (e.g. GitHub). See the Nature Portfolio guidelines for submitting code & software for further information.

Data

Policy information about availability of data

All manuscripts must include a data availability statement. This statement should provide the following information, where applicable:

- Accession codes, unique identifiers, or web links for publicly available datasets
- A description of any restrictions on data availability
- For clinical datasets or third party data, please ensure that the statement adheres to our policy

The data that support the findings of this study are not publicly available. Restrictions apply to the availability of these data, which were used under license for the

Research involving human participants, their data, or biological material

Policy information about studies with [human participants or human data](). See also policy information about [sex, gender (identity/presentation), and sexual orientation]() and [race, ethnicity and racism]().

Reporting on sex and gender	Sex was determined at birth. Findings apply to both sexes with sex included as a co-variate in all models. Sex-specific analyses were not performed due to small sample sizes in the high adversity group - this has been highlighted as a limitation of the study. The proportion of males and females were approximately equal in all datasets (Neuroimaging: Female = 51%, Male = 49%; Behavioral outcomes: Female = 52.5%, Male = 47.5%).
Reporting on race, ethnicity, or other socially relevant groupings	Ethnicity of the cohort was reported in the demographics table, but not included in the analysis. Ethnicity categories followed the major ethnic groups in Singapore (Chinese, Indian, Malay). Recruited participants (pregnant mothers) had homogeneous parental ethnic background. To examine the potential confounding effect of ethnicity, ethnicity was added as a co-variate in our analysis and findings remained unchanged (reported in Supplement S3b).
Population characteristics	Study data is from the Growing Up in Singapore Towards healthy Outcomes (GUSTO) birth cohort. Participants were recruited from two of Singapore's major public maternity units during pregnancy, and represent the general Singaporean population. The study population of the current study are offspring of the recruited participants (pregnant mothers). Neuroimaging data was collected over three study time-points: 4.5 years (range: 4.4 to 4.9); 6 years (5.8 to 6.6); 7.5 years (7.2 to 8.0). Behavioral outcomes were collected at age 7 years (range: 7.0 to 7.5).
Recruitment	The GUSTO study recruited pregnant women aged 18 years and above, attending their first trimester antenatal dating ultrasound scan clinic at Singapore's two major public maternity units, National University Hospital (NUH) and KK Women's and Children's Hospital (KKH), between June 2009 and September 2010. Participants were (i) Singapore citizens or permanent residents who were of (ii) Chinese, Malay or Indian ethnicity with homogeneous parental ethnic background, who (iii) had the intention of eventually delivering in NUH or KKH and (iv) intended to reside in Singapore for the next 5 years. Furthermore, (v) only women who agreed to donate birth tissues (including cord, placenta and cord blood) at delivery were included. Mothers receiving chemotherapy, psychotropic drugs or who had type I diabetes mellitus were excluded. It is possible that participants who agree to participate in the GUSTO study may be more conscious of scientific research.
Ethics oversight	The GUSTO study was approved by the National Healthcare Group Domain Specific Review Board (D/2009/021 and B/2014/00411) and the SingHealth Centralized Institutional Review Board (D/2018/2767 and A/2019/2406).

Note that full information on the approval of the study protocol must also be provided in the manuscript.

Field-specific reporting

Please select the one below that is the best fit for your research. If you are not sure, read the appropriate sections before making your selection.

☒ Life sciences　　　　☐ Behavioural & social sciences　　　　☐ Ecological, evolutionary & environmental sciences

For a reference copy of the document with all sections, see [nature.com/documents/nr-reporting-summary-flat.pdf]()

Life sciences study design

All studies must disclose on these points even when the disclosure is negative.

Sample size	For the current study, data has already been collected as it involves multiple time-points (from 4.5 years to 7.5 years). Therefore, sample size was determined by the data available. The total number of scans over the three time-points (N = 917) is one of the largest for pediatric neuroimaging cohorts, and equivalent to other published neuroimaging cohorts (e.g., PING) covering larger age ranges.
Data exclusions	Participants were excluded from analyses if there were incomplete/missing data, preventing the calculation of adversity scores and neuroimaging measures. Instead of data exclusions, a sensitivity analysis was conducted with exclusions based on neuroimaging motion criteria - main findings remain unchanged.
Replication	Findings were validated in two ways. First, the finding of accelerated development in the high relative to low adversity groups was validated with a different modality (DNA-derived biological age). Participants were included in this analysis as long as they had biological age data available at age 6, irrespective of whether they were included in the main analyses. Second, we compiled a small independent dataset of children with neuroimaging data, but incomplete adversity data (missing one category - the family assessment device). From this dataset, we included a small number of participants with adversity scores of 1 (representing the low adversity group), and adversity scores > 3 (representing the high adversity group) (n = 30 scans over two time-points). Numbers were small but we observed a similar trend to our main findings.
Randomization	Adversity groups were determined based on a cumulative adversity score (How many adversity categories a participant met criteria for). The cut-off for the high adversity group (>= 3) was pre-determined based on the Adverse Child Experience literature - where a cut-off of 3 or 4 is typically recommended.
Blinding	Adversity groups were assigned after data collection and processing. Thus, investigators were blinded during the data collection and processing stages.

Reporting for specific materials, systems and methods

We require information from authors about some types of materials, experimental systems and methods used in many studies. Here, indicate whether each material, system or method listed is relevant to your study. If you are not sure if a list item applies to your research, read the appropriate section before selecting a response.

Materials & experimental systems

n/a	Involved in the study
☒	☐ Antibodies
☒	☐ Eukaryotic cell lines
☒	☐ Palaeontology and archaeology
☒	☐ Animals and other organisms
☒	☐ Clinical data
☒	☐ Dual use research of concern
☒	☐ Plants

Methods

n/a	Involved in the study
☒	☐ ChIP-seq
☒	☐ Flow cytometry
☐	☒ MRI-based neuroimaging

Magnetic resonance imaging

Experimental design

Design type	Resting state
Design specifications	One run for each imaging modality
Behavioral performance measures	NA

Acquisition

Imaging type(s)	Functional, Diffusion
Field strength	3T
Sequence & imaging parameters	Resting State Site 1: gradient-echo planar imaging sequence sensitive to blood oxygenation level-dependent (BOLD) contrast; repetition time = 2660ms, echo time = 27ms, flip angle = 90 degrees, 3mm isotropic voxels, matrix size = 64 x 64 x 48, field of view = 192mm Resting State Site 2: gradient-echo planar imaging sequence sensitive to blood oxygenation level-dependent (BOLD) contrast; repetition time = 2620ms, echo time = 27ms, flip angle = 90 degrees, 3mm isotropic voxels, matrix size = 64 x 64 x 48, field of view = 192mm DTI site 1: single shot EPI sequence; repetition time = 8200ms, echo time = 85ms, 2mm isotropic voxels, matrix size = 96 x 96 x 69, field of view = 192mm DTI site 2: single shot EPI sequence; repetition time = 3572ms, echo time = 91.2ms, 2mm isotropic voxels, matrix size = 96 x 96 x 69, field of view = 192mm
Area of acquisition	Whole brain scan
Diffusion MRI	☒ Used ☐ Not used
Parameters	Site 1: 30 directions, b value = 1000 s/mm2, single-shell; Site 2: 30 directions per shell, b value = 1000, 2000, multi-shell. To harmonize with site 1, after cleaning and noise correction, only the b=0 and b=1000 diffusion gradients were extracted for use in probabilistic tractography

Preprocessing

Preprocessing software	Resting State: the CONN toolbox v20b - default preprocessing and denoising pipelines; Scan volumes with framewise displacement above 0.9mm or global BOLD signal changes above 5 standard deviations were identified as potential outliers. Both functional and anatomical data were resampled using 4th order spline interpolation. Functional data was smoothed using spatial convolution with a Gaussian kernel of 6mm full width half maximum (FWHM) DTI: Processed in FMRIB Software Library (FSL) v6.0.4
Normalization	ROIs from the yeo114 parcellation were normalized into subject T1 space using both linear and non-linear registration (FSLs FLIRT and FNIRT tools) before being transformed into subject specific diffusion space using FLIRT.

Normalization template	Functional and anatomical data were normalized into standard MNI space and segmented into grey matter, white matter, and CSF tissue classes using SPM12 unified segmentation and normalization procedure
Noise and artifact removal	Resting state: BOLD signal variance over time explained by nuisance variables was removed from the data using Ordinary Least Squares regression. BOLD time series were band-pass filtered to preserve only frequencies between 0.008 and 0.09 Hz.

DTI: All images were corrected for eddy currents which include susceptibility-by-motion interactions. Outlier slices are replaced with a Gaussian Process prediction with a set threshold of 3 standard deviations. The corrected data is then skull-stripped once more to provide a brain-tissue-only image which is further de-noised using a local PCA method. |
| Volume censoring | Resting state: First 4 volumes excluded to allow for magnetic field saturation. |

Statistical modeling & inference

Model type and settings	Statistical models performed in R - generalized additive models and linear mixed effects models
Effect(s) tested	Predictor - ScanAge by adversity groups (No, Low, High)

Specify type of analysis: ☐ Whole brain ☐ ROI-based ☒ Both

Anatomical location(s) | 114-region cortical atlas corresponding to 7 functional networks identified by Yeo et al. (Neuroimage. 2015;111:147-58), averaged over 114 regions for whole brain estimate, and over regions within a network for network estimate.

| Statistic type for inference
(See Eklund et al. 2016)	NA

Correction	NA

Models & analysis

n/a	Involved in the study
☐	☒ Functional and/or effective connectivity
☒	☐ Graph analysis
☒	☐ Multivariate modeling or predictive analysis

Functional and/or effective connectivity | Functional connectivity matrices were computed by measuring the bivariate correlation coefficients of the BOLD time series between each seed and target ROIs through a haemodynamic response factor (hrf)-weighted general linear model. Structural connectivity matrices were computed by calculating streamline densities between each seed and target ROIs derived from probabilistic tractography using FSL's BEDPOSTX and PROBTRACKX tools